EINDHOVEN UNIVERSITY OF TECHNOLOGY

Department of Applied Physics

Research group of Materials Simulation and Modelling

CLASSICAL FORCE FIELDS FOR DOPED HEMATITES

J.M.C. DELLEVOET 1354264

BACHELOR FINAL PROJECT (3CBX0)

APPLIED PHYSICS

SUPERVISORS

S. CALERO

J.J. GUTIERREZ-SEVILLANO

REPORT NR. R-0008-B

FEBRUARY, 2022

EINDHOVEN UNIVERSITY OF TECHNOLOGY

Abstract

Hematite has long been a material of interest to use in photoelectrochemical cells in order to produce hydrogen from solar energy. However, one of the main challenges is the poor conductivity of hematite, which makes that the reaction of splitting of water cannot be fully completed without using an overpotential. One solution could be to introduce dopants into the hematite such that the conductivity is improved. In this report we investigated three of such doped hematites, with the dopants being cobalt, nickel and titanium. We tried to fit the parameters of the classical force fields of the three doped hematites such that the energy curve of the binding energy resembles that of DFT calculations. We found that not only the parameters of the interaction between the dopant and the water needed to be fitted, but also the other interaction parameters of the hematite with the water needed to be refitted. In this way we found a set of parameters that can represent the interaction of the doped hematites with a water molecule. We concluded that the introduction of the dopant changes the interaction of the rest of the hematite with the water, and this does not seem to depend on the type of dopant. Only the parameters of the dopant need to be refitted for new dopants.

Contents

1 Introduction **3**
- 1.1 Splitting water . . . 3
- 1.2 Hematite . . . 4
- 1.3 DFT calculations . . . 5
- 1.4 Modeling and force fields . . . 6
- 1.5 Molecular dynamics . . . 6

2 Objectives **8**

3 Methods **9**
- 3.1 Water model . . . 9
- 3.2 Hematite models . . . 10
  - 3.2.1 Pure hematite . . . 10
  - 3.2.2 Doped hematite: Cobalt . . . 10
  - 3.2.3 Doped hematite: Nickel . . . 11
  - 3.2.4 Doped hematite: Titanium . . . 12
- 3.3 Force fields . . . 12

4 Results and discussion **14**
- 4.1 Placement of the water molecule . . . 14
- 4.2 Fitting the dopant interaction parameters . . . 16
- 4.3 Fitting two sets of four parameters . . . 18
- 4.4 Fitting six parameters . . . 21
- 4.5 Fitting nickel and titanium . . . 22
- 4.6 Molecular diffusion . . . 23

5 Conclusion **25**

A Diffusion **27**

1 Introduction

With climate change becoming a consistently growing problem in the present day, many scientists, activists and policy makers try to find solutions to both reduce climate change, but also preserve or improve our current way of living. One solution that has sparked the interest of scientists is the use of hydrogen as source of fuel for vehicles, and as storage possibility for energy. The last is especially useful because it eliminates the use of excessively large batteries, which also cost precious metals to produce.

The materials that are needed for hydrogen production, especially when choosing the right ones, are much more accessible. The main material for producing hydrogen is water. This water can be split by applying energy, usually in the form of an electrical current, to a water molecule such that the molecule decomposes into hydrogen and oxygen. Of course, this energy needs to come from a renewable source itself, otherwise the whole process would be non-efficient, due to conservation of energy. Therefore, research has been done into using solar cells that can use the energy of the sun for the splitting of water and thus the production of hydrogen.

One material that can be used for this purpose is so-called hematite α-Fe_2O_3, which is a crystal that is commonly available, is stable in aqueous solutions and has a small bandgap of 1.9-2.2 eV. Some of the challenges that this innovation still faces are poor conductivity and lacking knowledge about the interaction between water and the hematite. The first might be solvable by doping the hematite, such that it becomes a p-type or n-type semiconductor. Quantum mechanical calculations for these type of hematites show promising results [1]. The second challenge might be solvable by optimizing parameters of classical calculations such that the interaction energies follow quantum mechanical values [2]. The latter is namely more accurate than classical calculations, but is not suitable for large systems of atoms. Therefore, by optimizing the parameters of the classical calculations, the system of atoms can be expanded beyond the boundaries of quantum mechanical calculations.

1.1 Splitting water

One can argue that water is the most important molecule when it comes to life on Earth. Even though the water molecule looks simple at first, it holds some unique properties that for example cause ice to float on water [3]. Figure 1 depicts a schematic representation of a water molecule. It consists of two hydrogen atoms, bonded by an oxygen atom, which sits at an angle with the two hydrogen atoms.

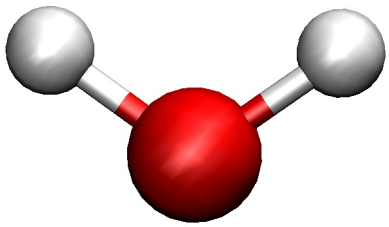

Figure 1: *A schematic representation of a water molecule. The red sphere represents an oxygen atom and the two white spheres represent hydrogen atoms. Figure generated using [4].*

This molecule has a dipole moment, and can therefore form hydrogen bonds between water molecules, mostly in liquid water. This has as a result that water is hard to model and different types of research need different models that can represent a water molecule.

When energy is applied to water molecules, they can break down into hydrogen and oxygen atoms, which then form H_2 and O_2. This chemical reaction can be written as follows:

$$2\,H_2O \longrightarrow 2\,H_2 + O_2. \tag{1}$$

The hydrogen that is released in this reaction can be stored and then burned as fuel in the opposite reaction.

1.2 Hematite

The solar cells that we consider in this report have as main reactive material pure and doped hematites. Hematite is a crystalline material, which is made up out of iron oxide Fe_2O_3, denoted by α-Fe_2O_3. It is available in nature, and pure hematite is relatively low in price. This pure hematite has a bandgap of 1.9-2.2 eV, which is a good bandgap for breaking down water molecules. A snapshot of the surface of pure hematite is shown in Figure 2.

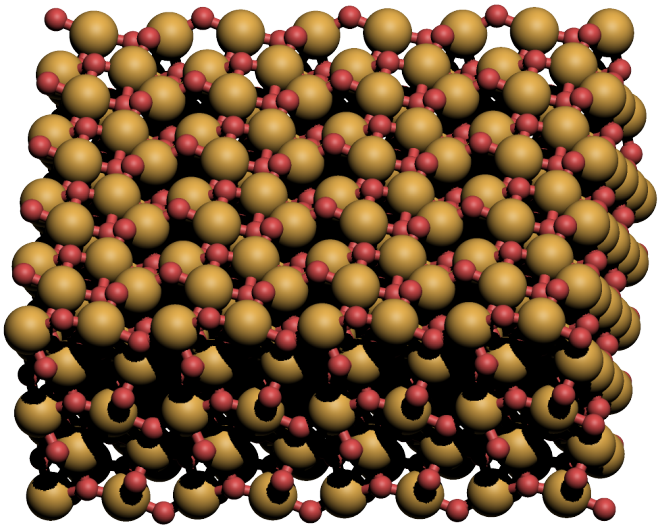

Figure 2: *A section of the surface of pure hematite, where the red spheres represent oxygen atoms and yellow spheres represent iron atoms. Figure generated using [5].*

Another advantage of hematite is that it is stable by itself, even in aqueous environments, and will therefore not break down when exposed to water molecules. The hematite can absorb 40% of the sunlight, and it decomposes water in the following two subreactions:

$$\begin{aligned} 2\,H_2O + 4\,h^+ &\longrightarrow 4\,H^+ + O_2 \\ 2\,H^+ + 2\,e^- &\longrightarrow H_2, \end{aligned}$$

where h^+ is a hole in the valence band and e^- an electron in the conduction band of the hematite [6]. However, the conductivity of hematite is by itself not high enough to complete the water splitting reaction, i.e. additional electrons are needed to complete the reaction. Therefore, the surface of hematite can be doped in order to obtain a material that can complete the water splitting reaction without applying an external bias. This improves the conductivity, which can make the doped hematite more suitable for water splitting [1].

1.3 DFT calculations

A very accurate method to determine energies in a force field is density functional theory (DFT). This method uses quantum mechanical theory to try to find the exact interaction of nuclei and electrons in a many-body system. Such a system is described by the Schrödinger equation for each body in the configuration. The total Hamiltonian is then given by [7]:

$$\hat{H} = T_e\left(\{\vec{r}_i\}\right) + T_n\left(\{\vec{R}_l\}\right) + V_{n-n}\left(\{\vec{R}_l\}\right) + V_{e-n}\left(\{\vec{r}_i\},\{\vec{R}_l\}\right) + V_{e-e}\left(\{\vec{r}_i\}\right), \tag{2}$$

where the sets $\{\vec{r}_i\}$ and $\{\vec{R}_l\}$ denote the set of coordinates for the electrons and nuclei, respectively. The term T_e denotes the kinetic energy of the electrons, T_n the kinetic energies of the nuclei and the V_i terms denote the three different potential energies between the bodies.

For a many-body system, this equation is too complex to solve with modern-day technology and techniques. Hence, approximation methods have been developed that simplify the Hamiltonian and can therefore find numerical solutions of equation (2) of high accuracy [8]. One of these methods is the DFT method.

The first approximation that the DFT method makes is taking the nuclei in the configuration as fixed, which is called the Born-Oppenheimer approximation. This is justified by the fact that the nuclei, even the lightest ones, are far more heavy than the electrons. These fixed nuclei will however cause an external potential field for the electrons. This approximation will thus cause $T_n = 0$, $V_{n-n} = 0$ and the term $V_{e-n}\left(\{\vec{r}_i\},\{\vec{R}_l\}\right) = V_{ext}\left(\{\vec{r}_i\}\right)$ in equation (2), so that the Hamiltonian is only dependent on the positions of the electrons in the fixed external potential field, the interaction between electrons and their respective kinetic energies.

After this approximation, the Hamiltonian is still complex, because it involves the interaction potential for all the electrons. The DFT method introduces the electron density in order to simplify the problem further. For a given normalized state Ψ of the system, this density is given by:

$$n(\vec{r}) = N_e \int \left|\Psi(\vec{r}_1,...,\vec{r}_{N_e},\sigma_1,...,\sigma_{N_e})\right|^2 d\sigma_1,...,d\sigma_{N_e}, \tag{3}$$

where the σ_i is the spin of the electron with coordinate $\vec{r}_i$ and N_e is the total number of electrons. Using this density function for the ground state of the system, one can calculate the energy of the system. For example, the Thomas-Fermi model states that the energy is then given by:

$$E[n(\vec{r})] = \frac{3}{10}(2\pi^2)^{2/3}\int n^{3/5}(\vec{r})d\vec{r} - Z\int\frac{n(\vec{r})}{\vec{r}}dr + \frac{1}{2}\int\int\frac{n_1(\vec{r})n_2(\vec{r})}{|\vec{r}_1-\vec{r}_2|}d\vec{r}_1 d\vec{r}_2 \tag{4}$$

We now assume that there is a one-to-one relation between the external potential and the electron density, i.e. an external potential will uniquely determine the electron density $n(\vec{r})$ and vice versa. The DFT calculates the ground state of the electron density as follows:

1. Start with an initial guess of the electron density $n(\vec{r})$.
2. Calculate the subsequent potential $V_s(n(\vec{r}))$. This is possible, since the relation is one-to-one. This single-particle potential is the potential that is experienced by an electron, and it depends on the electron density and the coordinates of the electron in question.
3. The effective potential can be used to calculate the Kohn-Sham orbitals by means of the Kohn-Sham equations, given by
$$\left(-\frac{\hbar}{2m_e}\nabla^2 + V_s[n(\vec{r})]\right)\psi_i = \varepsilon_i\psi_i. \tag{5}$$
4. Using these orbitals ψ_i the electron density can be recalculated, using
$$n(\vec{r}) = \sum_{i=1}^{N_e}\left|\psi_i\right|^2.$$

5. Use this new electron density to repeat steps 2-4 until convergence is reached.

The electron density that follows from this algorithm is the ground state density, for which the total energy is minimized. The calculation of this ground state energy is in this report done using the VASP package [9, 10]. This ground state density can then be used to calculate the binding energy between water and hematite.

1.4 Modeling and force fields

In this report, we consider the interaction energy between water molecules and (doped) hematite, in order to understand how the water interacts with the hematite surface.

We know that the potential energy of any molecule or structure is given by

$$V = V_{bonded} + V_{non-bonded}, \tag{6}$$

where

$$V_{bonded} = V_{bond-stretch} + V_{angle-bend} + V_{torsion}$$

and

$$V_{non-bonded} = V_{vanderWaals} + V_{electrostatics}.$$

In this report, we only consider non-bonded energy, since we want to know the potential energy of a water molecule in presence of hematite, which is always a non-bonded potential. For the electrostatic potential we use the well-known Coulombic potential. This potential is given by

$$V_{electrostatic} = \frac{1}{4\pi\varepsilon_0}\frac{q_i q_j}{r_{ij}}, \tag{7}$$

where ε_0 is the permittivity of vacuum, q_i and q_j are the charges of the particles between which the potential is calculated and r_{ij} is the distance between these two particles, respectively.

The van der Waals potential has several approximations, and in this report we work with the so-called Buckingham potential. The van der Waals potential is then approximated with the following equation:

$$V_{vanderWaals} = Ae^{-r_{ij}/\rho} - Cr_{ij}^{-6}. \tag{8}$$

In this equation, A, ρ and C are parameters which differ for the different pairs of type of atoms i, j and r_{ij} is the distance between one such pair of atoms for which the potential is calculated.

In order to model the interaction between water and (doped) hematite, we need to choose how the charges in the different atoms are defined. For example, we can consider a water molecule as two spheres with different charges, one representing the oxygen atom and the other representing the two hydrogen atoms combined. However, we can also consider three spheres with different charges, one for each atom in the water molecule. In Section 3, more details are given about the models for water and hematite that are used in this report.

When these models are determined, the parameters for the van der Waals potential need to be determined. By optimizing these parameters such that the consequent binding energies imitate the energies found using DFT calculations, we can extend the calculations to a bigger section of the hematite and a larger number of water molecules, without losing accuracy in the calculated binding energies.

1.5 Molecular dynamics

Once the force fields of the hematite is known, i.e. the parameters are accurately determined, it can be used to simulate water molecules in the presence of hematite. Molecular dynamics can be used to simulate the movement of particles. It usually uses Newtons laws of motion to calculate the movement of the particle. Since the force field is known, the forces on particles can be

calculated and therefore also the movement of the particles at an instantaneous moment in time. This simulation can therefore not be done in a continuous way, but must be done with discrete time steps. The typical timescale of such simulations is a few or a fraction of nanoseconds, such that a typical time-step is a fraction of a picosecond. By taking the positions of the particles for each time-step, an animation can be made of how the particles interact with each other and how they move.

An important parameter to measure the amount of movement of molecules is the diffusion coefficient [11]. This parameter is calculated from the mean square displacement (MSD) of single particles and is given by:

$$D^{\alpha} = \frac{1}{2N} \lim_{t \to \infty} \left\langle \sum_{i=1}^{N} \frac{d}{dt} \left(r_{i\alpha}(t) - r_{i\alpha}(0) \right)^2 \right\rangle, \tag{9}$$

where α represents one of the three Cartesian directions, i.e. $\alpha = x, y$ or z, N is the number of molecules in the system and t is the time. The last parameter, $r_{i\alpha}$ represents the α component of the center of mass of the molecule labeled i. The diffusion coefficient is thus a half times the slope of the MSD curve as function of the time. These diffusion coefficients are calculated in the range where the MSD has values between $(0.5\lambda)^2 - \lambda^2$, where λ is the width of the cage, which in this report is represented by one dimension of a unit cell of the hematite.

2 Objectives

This report is an extension of the research conducted in [2]. There, the interaction between pure hematite and a water molecule is investigated. The parameters of the force field between water and pure hematite are fitted so that the consequent energy curves follow the DFT energy curves the most accurate.

In this report, the goal is the same as for the pure hematite. We want to fit the parameters of the classical force field such that the energy curves of the water near the surface of the dopant hematites follow those of the DFT calculations. These parameters can then be used for larger calculations, since the DFT calculations are not suited for this due to the large computational cost.

We first look at how the energy wells on the surface are affected by the introduction of the dopants. Water molecules that are near the surface are attracted by these energy wells, and the positioning and depth of these wells thus affects the movement of the water molecules. We can also use these wells to find the energy curve of the water molecule that moves towards this well as a function of the distance between the water and the hematite.

After this, we want to determine the number of parameters that are needed to fit the energy curves to the DFT curve. We initially only fit the parameters introduced by the dopant-water interaction, but more parameters might be needed to fit the energy curves. This is because the other interactions between the hematite and the water might also be affected by the introduction of the dopant. But we also have that the more parameters need to be fitted, the bigger the computational cost. Therefore, we want to minimize the number of parameters that are needed to accurately fit the DFT curve. The parameters that we find that are needed to fit the curves can then be used to fit the energy curves to represent the DFT energy curves.

The second aim of this report is to find the diffusion coefficients for different numbers of water molecules over the surface of pure hematite. We use the fitted pure hematite field from [2] to run simulations to calculate the MSD values in the plane parallel to the surface of the hematite. These MSD values can then be used to calculate the diffusion coefficients. These coefficients indicate the amount of movement of the water molecules near the surface.

3 Methods

In this section, the models for the water molecule and the crystalline structures are described.

In [2] it was found that using point charge models for both the surface and the water molecule could represent the energies of DFT calculations fairly accurately, at least compared to the more complex core-shell charges model. These point charge models are therefore also used in this report, such that the different models for the doped hematites can not only be adjusted to represent the DFT calculations, but can also be compared to each other.

All individual models and their relevant parameters are described in this section, and in Section 3.3, the interaction of the water molecule and the different hematites is described with their relevant interaction energies. These models and their interactions are then used to calculate the potential energy of the water molecule in the presence of the different hematites using the RASPA code.

3.1 Water model

As mentioned earlier, the model for water that is used in this report, is a point charge model called the extended simple point charge (SPC/E) model [12]. This model takes three point charges, of different magnitudes, at the places of the oxygen and the two hydrogen atoms, respectively. It then treats the molecule as rigid, such that the point charges have a fixed distance with respect to each other.

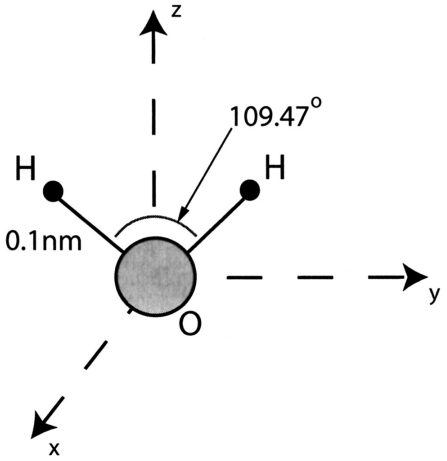

Figure 3: *A schematic depiction of the water molecule according to the SPC/E model. Source: [12].*

The equilibrium position of the water molecule assumes that the angle between the two hydrogen atoms is 109.47° and both their distances to the oxygen atom to be 0.1 nm. This is schematically depicted in Figure 3, where the scaling of the atoms is exaggerated for clarity. The magnitudes of the point charges are $-0.8476e$ for the oxygen atom and $0.4238e$ for each of the two hydrogen atoms.

There also exist other models for a water molecule that can be more or less complex than the SPC/E model, and can simulate different properties of the water more accurately than other models. However, in this report the interaction of the water molecule in the proximity of doped hematites is compared to the behavior close to the non-doped (110)-hematite. Since the parameters of the force field mentioned in Section 1.4 are already optimized [2], these parameters and the same model for water can be used to compare the different doped hematites. The results in [2] also show that this model can relatively accurately represent the binding energies that are

calculated using the DFT method. Therefore, we assume that this model can also be used to accurately represent the DFT energies for doped hematites.

3.2 Hematite models

3.2.1 Pure hematite

In order to compare the doped hematites to the pure hematite, the pure hematite must be defined first. In that way, the doped hematites follow by exchanging some atoms in the crystalline structure. In this report, the hematite that is considered is the (110) surface of a rhomboedral cell of hematite. This structure is made up out of oxygen and iron atoms, which together form a crystalline structure. Figure 4 depicts this surface schematically.

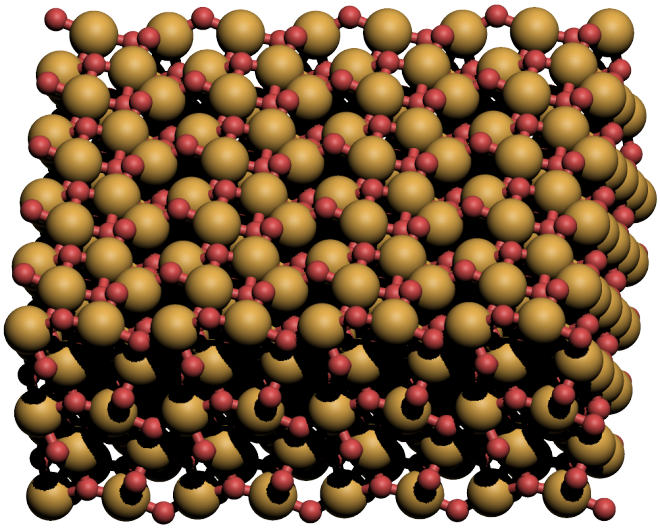

Figure 4: *A schematic depiction of pure hematite. The red spheres represent oxygen atoms and the yellow spheres represent iron atoms. Figure generated using [5].*

Every atom in the crystalline structure is modelled with a point charge of a certain magnitude. This charge depends on the type of atom and the position of the atom itself. The magnitude of the hematite section that is considered is 29.43784 Å$\times$ 26.99145 Å. The distances between atoms are calculated using the DDEC6 scheme, which in this case assumes that the eight middle layers of the section of hematite that is considered are fixed and two layers on opposite sides are allowed to relax. The forces on the atoms in the outer layers are then allowed to relax until the force on the atoms were less than 0.03 eV/Å. After this calculation, we assume that the atoms are at fixed distances with respect to each other, also when brought into contact with water molecules.

3.2.2 Doped hematite: Cobalt

For the cobalt doped hematite, four of the iron atoms in the top layer of the hematite are replaced by a cobalt atom. These iron atoms are all located at the very top of the layer and the cobalt atoms also sit in the top layer of the hematite. A schematic depiction of this doped hematite is shown in Figure 5.

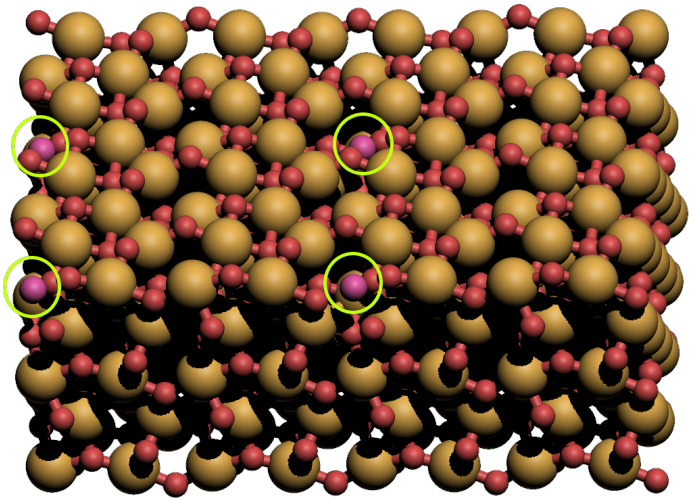

Figure 5: *A schematic depiction of cobalt doped hematite. The red spheres represent oxygen atoms, the yellow spheres represent iron atoms and the pink spheres represent the dopant cobalt, indicated by the green circles. Figure generated using [5].*

In this figure, the pink atoms represent the cobalt atoms that replace the iron atoms. These cobalt atoms are also modelled using a point charge, which is different from the charge of the former iron atom. They also have a bigger atomic mass than the iron atoms. The latter have an atomic mass of 55.845 u while the cobalt atoms have a mass of 58.9332 u in our model. Since these two characteristics of the atom have changed, the forces in the structure and the relative distances between atoms will also change in the top two layers of the hematite. These distances are therefore recalculated using the same scheme as the pure hematite, namely the DDEC6 scheme. The dimensions of the surface of this unit cell of doped hematite are 29.70463 Å$\times$ 21.78885 Å.

Cobalt is one group higher in the periodic table of elements than iron and is thus an *n*-type dopant, providing additional electrons to the hematite. It has been shown that this type of doping can improve the conductivity and photoelectrical activity for other types of *n*-type dopants. This suggest that cobalt doping can also lead to these effects. It can also reduce the amount of overpotential that is needed for water splitting [13].

3.2.3 Doped hematite: Nickel

Similar to the cobalt doped hematite, nickel doped hematite replaces four of the iron atoms in the surface of the hematite in the section of hematite we consider. This new structure is schematically shown in Figure 6, where the nickel atoms are represented by the dark pink spheres. The dimensions of this new structure are 29.70463 Å$\times$ 21.78885 Å. Nickel has an atomic mass of 58.6934 u in this model, and also the point charge of the nickel is different from the iron, such that the relative distances change again. The structure is recalculated with the DDEC6 scheme to find the new distances.

Compared to iron, nickel is two groups higher in the periodic table of elements and is therefore also an *n*-type dopant for the hematite. It has been shown that nickel doping can also enhance the conductivity of pure hematite [14].

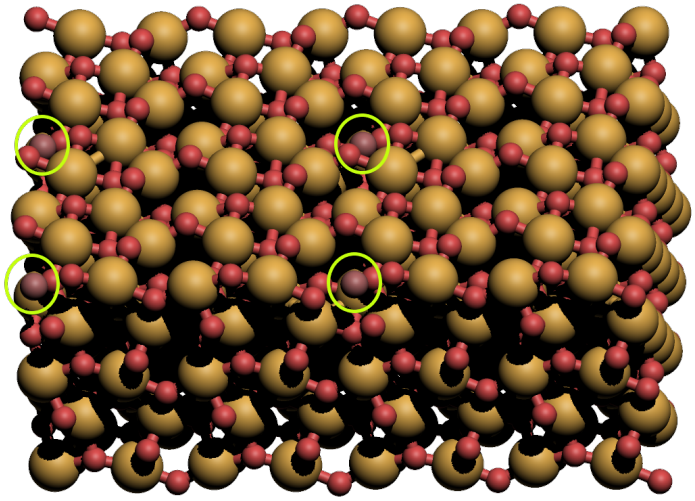

Figure 6: *A schematic depiction of nickel doped hematite. The red spheres represent oxygen atoms, the yellow spheres represent iron atoms and the dark pink spheres represent the dopant nickel, indicated by the green circles. Figure generated using [5].*

3.2.4 Doped hematite: Titanium

The last dopant that we consider in this report is titanium. This element is four groups lower in the table of elements, but is also a n-type dopant for the hematite [1]. This type of hematite has already been produced and studied, and it is not a higher conductivity that makes that titanium doped hematite is a better solar cell than pure hematite, but probably the passivation of defects in the hematites surface due to the introduction of the titanium dopant [15].

Like for the cobalt and nickel doped hematites, four of the iron atoms in the original pure hematite section are replaced by titanium atoms. The resulting hematite surface section is shown in Figure 7, where the light blue spheres represent the inserted titanium atoms. The relative internal distances are recalculated using the DDEC6 scheme and the dimensions of the section are now 29.70463 Å$\times$ 21.78885 Å.

3.3 Force fields

The last thing we use in order to model the interaction, are the interaction energies between atoms. Following the reasoning from Section 1.4, we want to calculate the non-bonded energies between atoms, which is the sum of the electrostatic and van der Waals potential. The electrostatic potential between atoms labeled i and j is modelled using the Coulombic potential, which is given by

$$V_{Coulomb} = \frac{1}{4\pi\varepsilon_0}\frac{q_i q_j}{r_{ij}}, \tag{10}$$

where q_i and q_j are the charges of the atoms labeled i and j and the variable r_{ij} is the distance between these atoms. The values of the point charges of the atoms in both the hematite and the water molecule are input parameters of the simulation. Also, the distance r_{ij} will depend on the placement of the water molecule above the hematite. Therefore, this potential has no parameters

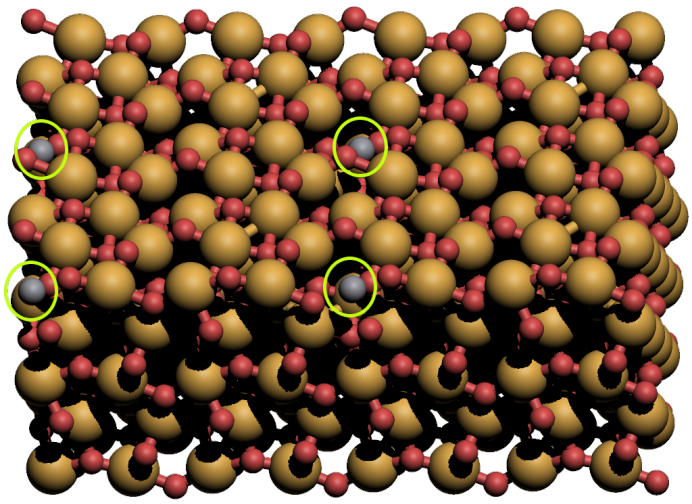

Figure 7: *A schematic depiction of titanium doped hematite. The red spheres represent oxygen atoms, the yellow spheres represent iron atoms and the light blue spheres represent the dopant titanium, indicated by the green circles. Figure generated using [5].*

that can be adjusted for a given position of a water molecule and the given models of the different hematites and water molecules.

The second term in the non-bonded potential is the van der Waals potential. In this report, we model this potential using the Buckingham potential. For two atoms label i and j, this potential is given by

$$V_{Buckingham} = Ae^{-r_{ij}/\rho} - Cr_{ij}^{-6}, \tag{11}$$

where the variable r_{ij} is again the distance between atoms i and j. The parameters A, ρ and C depend on the type of atoms that i and j are. These parameters have already been optimized to fit the DFT values for pure hematite [2], and these values can be found in Table 1. Initially, we assume that these fitted parameters do not change when a dopant is introduced. The parameters of the dopant are initially taken to be the values found in Table 1. These initial parameters of the doped metals interacting with the water are not of great importance, since these are the parameters which we want to adjust to fit the DFT calculations. However, their magnitudes still need to be reasonable in order to get a good idea of the binding energies on the surface of the hematite.

Table 1: *The initial parameters of the force field between doped hematites and water molecules.*

Interaction	A (eV)	ρ (Å)	C (eV Å^6)
$O_{hematite}$-O_{water}	34146.0	0.149	28.92
$Fe_{hematite}$-O_{water}	551.25	0.439867	0.0
$O_{hematite}$-H_{water}	495.3375	0.166667	0.0
$(Co/Ni/Ti)_{hematite}$-O_{water}	684.905 [16]	0.5	0.0

Using these two potential energies, the binding energy of water to the hematite can be calculated for a given position of the water with respect to the surfaces.

4 Results and discussion

This section describes all the steps and intermediate results that we obtained while fitting the energy curves of the classical force field to the energies obtained using DFT calculations. Also, we discuss the conclusions that follow from these results and the subsequent steps that follow from the intermediate results. We started by analyzing the three different dopant hematites, but after the first fitting, we only analyzed the cobalt doped hematite due to time restrictions. Once we fitted the parameters of the cobalt doped hematite, we used the knowledge from this fitting to fit the other two doped hematites.

4.1 Placement of the water molecule

The first step of trying to parameterize the classical force field into one that resembles DFT calculations, was scanning the surfaces of the doped hematites. To do this, we set one water molecule at a given distance away from the surface and translated it in the parallel plane of the surface. These translations over the three doped hematites gave energy landscapes over the surfaces, shown in Figure 8, and it thus shows energy wells where the forces on the water molecule are attractive. In these figures, the red peaks represent positive energies, which are repulsive, and the purple and blue valleys represent negative energies, which are attractive.

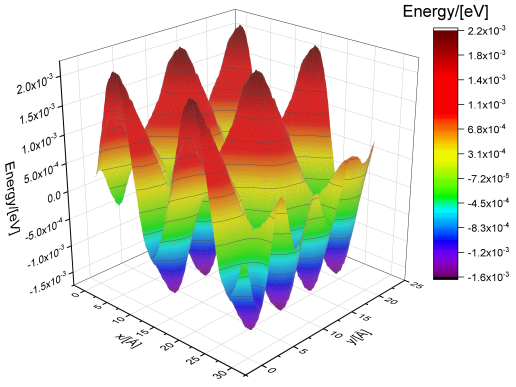

(a) *The energy landscape of the cobalt doped hematite.*

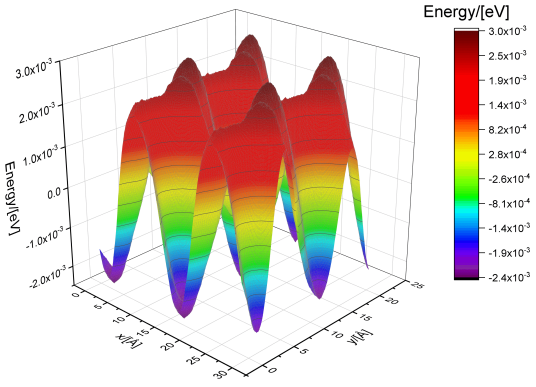

(b) *The energy landscape of the nickel doped hematite.*

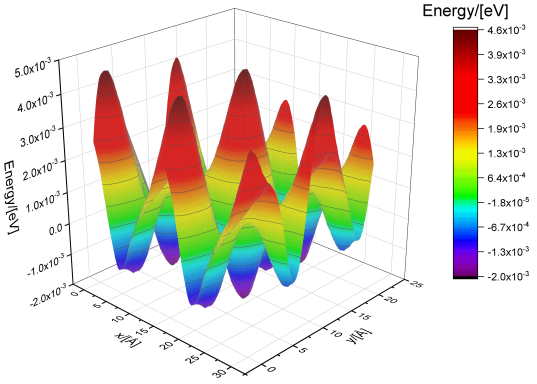

(c) *The energy landscape of the titanium doped hematite.*

Figure 8: *The energy landscapes of the three different doped hematites. In these figures, red denotes a higher, positive energy and purple denotes a lower, negative energy.*

A water molecule sits on a spot on the hematite surface where there is an energy minimum. There were multiple energy minima for every surface, and we chose to place a water molecule in a minimum that is closest to a dopant atom, since we wanted to investigate the influence that this dopant has on the force field of the hematite and the energy curve of the water molecule. There are oxygen atoms in the surface of the hematite, where these energy wells are located. These oxygen atoms also cause energy minima for pure hematite. Therefore, we placed the water molecule on top of the oxygen atom in the well, where one of the hydrogen atoms of the water molecule points towards the surface. We started with a distance of 1Å between the hydrogen of the water and the oxygen of the hematite, after which we moved the water molecule orthogonally away from the surface to a distance of 4Å for the cobalt and titanium doped hematite and a distance of 5Å for the nickel doped hematite.

By calculating the energy at discrete distances between the hematite and the water molecule, we obtained the potential energy of the water as function of the distance between the water and the surface. These initial curves are the figures show in Figure 9.

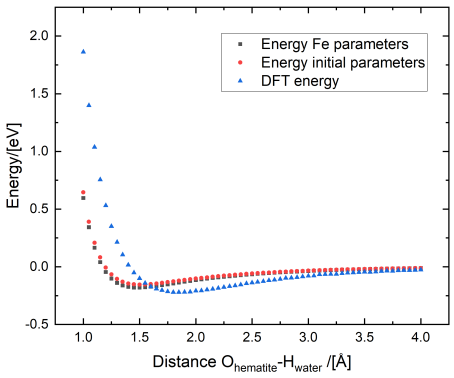

(a) *Cobalt*

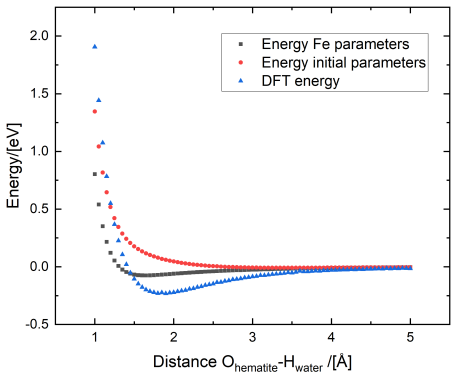

(b) *Nickel*

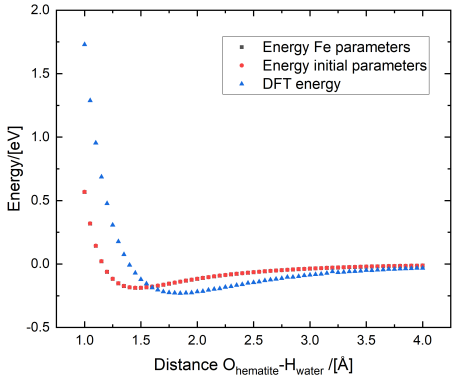

(c) *Titanium*

Figure 9: *The energy curves for the different doped hematites. In each figure, the curves of the initial parameters and the iron parameters are compared with the DFT energies.*

In these figures we plotted the energy curve of the initial parameters from Table 1, the DFT energies, and also the energy curve where we take the parameters of the dopant metal with the oxygen of the water equal to the iron parameters with the oxygen of the water from Table 1. We could see from these figures that although changing the parameters does transform the curves, they both

do not resemble the DFT energy curves for any hematite. The minima of the classical curves are at a different distance than the DFT energy curve, and also the magnitudes of the minima differ depending on the choice of parameters. Therefore, we tried to alter the interaction parameters of the different doped atoms with the oxygen of the water in order to obtain energy curves that fit the DFT energy curves more accurately. From this point on we took the parameters of the interactions as shown in Table 2, and we fit these parameters by multiplying them by factors.

Table 2: *The parameters that are used to fit the classical force fields of the doped hematites.*

Interaction	A (eV)	ρ (Å)	C (eV Å^6)
$O_{hematite}$-O_{water}	34146.0	0.149	28.92
$Fe_{hematite}$-O_{water}	551.25	0.439867	0.0
$O_{hematite}$-H_{water}	495.3375	0.166667	0.0
$(Co/Ni/Ti)_{hematite}$-O_{water}	551.25	0.439867	0.0

4.2 Fitting the dopant interaction parameters

We proceeded by trying to fit the parameters A and ρ from equation (11) between the dopant metal and the oxygen of the water. We assumed that $C = 0.0$ for the dopant metals, like it was fitted between the pure hematite iron and the oxygen of the water. Experience showed that this parameter has little to no influence on the fitting of the curve. We also assumed that the parameters for the three other interactions, that were fitted for the pure hematite, were not altered by introducing the dopant metals. We thus had two parameters to fit, which we did by first taking the parameters of iron as initial parameters and then multiplying both A and $1/\rho$ independently by a factor, initially between 0.1 and 1.9, but the factors and steps in between factors varied throughout the fitting. In this way, we created a grid of parameters for which we could calculate the energy curves.

The way we compared these energy curves to the DFT calculations was by calculating the square distance between the DFT energy and the classical energy for every measurement point of the energy, i.e. for every distance between the hematite and the water. By summing this over all the measurement points, we had one parameter that determined how well the calculated energy curve fitted the DFT energy curve. We called this parameter the sum of square distances (SSD) of the given doped hematite, and we wanted to minimize this parameter by adjusting the parameters.

The calculation of the SSD was done for every energy curve on the parameter grid to find the set of parameters that fitted the DFT curve the best according to the sum of the square distances. In this way we obtained plots like the one shown in Figure 10, where the SSD is plotted as a function of the factor used for A and the factor used for $1/\rho$. The purple again shows the lower values and the red shows higher values of the SSD for the given parameter grid.

We found that the minimum of the SSD seemed to lie outside of the grid we initially chose, because the minimum of the grid was on the border of the chosen grid. We then translated and refined the grid to find the minimum. However, the minimum again seemed to lie outside the grid. After a few translations we could not find the exact minimum of the SSD, and the SSD looked like it was always decreasing towards the border of the grid. Furthermore, if we plotted an apparent minimum of one of the grids, i.e. a grid point on the edge of the grid, the resulting energy curve that followed from these parameters showed the behavior shown in Figure 11, where we plotted some apparent minima of some of the grids of cobalt doped hematite. These apparent minima have a positive energy curve, which means that the water experiences no attractive forces. The SSD for these curves is of the order of 2-3 eV^2. The figures shown in Figure 11 are the energy curves for cobalt doped hematite, but the nickel doped and titanium doped hematite showed the same behavior in the apparent minima and translating of the grid.

From these comparisons, we suspected that the parameters might not be able to shift the minima of

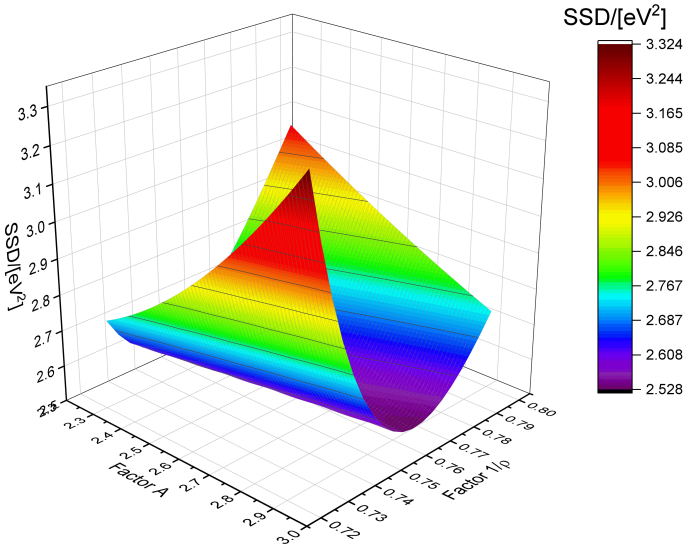

Figure 10: *An example of a parameter grid with the sum of square distances (SSD) between classical curves and the DFT energy curve of cobalt doped hematite as function of the grid.*

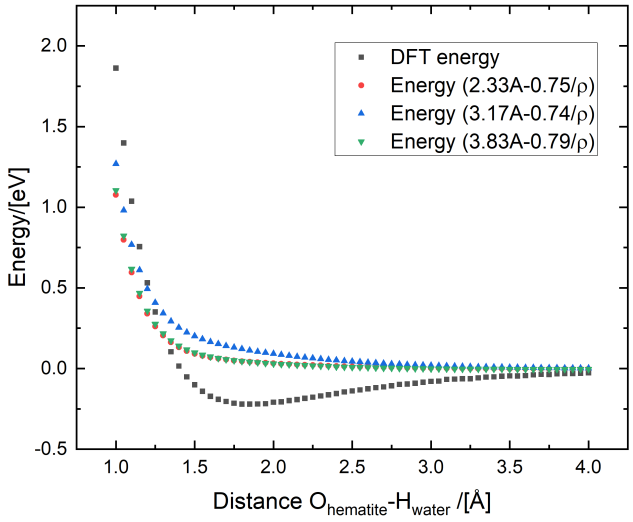

Figure 11: *A comparison of the DFT energy with some of the apparent minima of the SSD after translating the parameter grid of cobalt.*

the energy curves from Figure 9 to the left or right, but can only move them up or down, or let the minima disappear entirely like in Figure 11. To confirm these suspicions, we tried to investigate the effects that changing one of the two parameters has on the resulting energy curve, while keeping the other constant. This resulted in the plots of Figure 12 for the cobalt doped hematite. Figure 12a shows the effect of the parameter A by multiplying A by a factor between 0.1 and 1.9 while keeping $1/\rho = 2.27342$ Å^{-1}. Figure 12b is the effect of the parameter ρ by multiplying $1/\rho$ by a factor between 0.1 and 1.9 while keeping $A = 551.25$ eV.

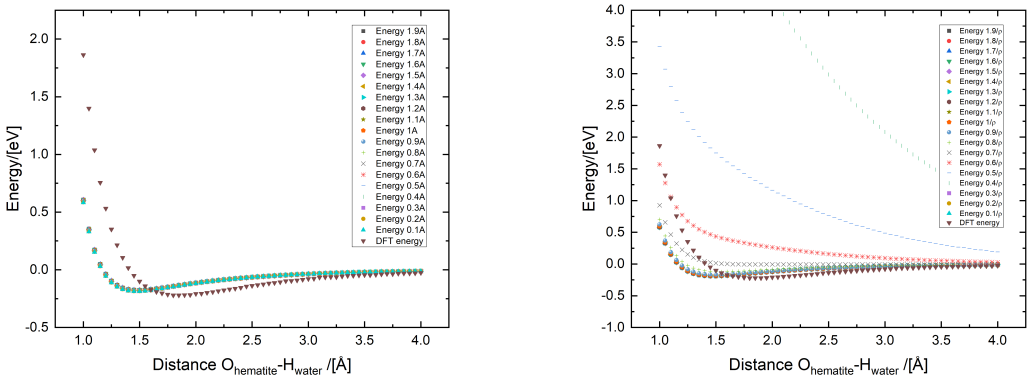

(a) *A comparison of the influence of the parameter A on the energy curve.*

(b) *A comparison of the influence of the parameter ρ on the energy curve.*

Figure 12: *The comparison of the influence of the different parameters of the cobalt-water interaction on the energy curves.*

From these figures, we saw that both parameters cause the energy curves to shift up and down, but the minimum is barely shifted left or right. We therefore concluded that it would probably not be possible to fit the force field of the hematites to the DFT curves using only the two parameters of the dopant metal and water interaction. Of course, in this way we may have neglected some combination of values for A and ρ, but we tried to fit these parameters and that also did not result in a good fitting of the energy curve.

Again, we showed the influence of the parameters of the cobalt-water interaction, but the influence of the nickel-water and titanium-water interactions also show the same behavior as the behavior depicted in Figure 12 for their respective force fields.

4.3 Fitting two sets of four parameters

Next, we tried incorporating more parameters into the fitting of the curves. We did this because we suspected that the introduction of the dopant might alter the interaction of the other atoms in the hematite with water as well. We took two sets of four parameters each and fitted them in parallel, and did this only for the cobalt doped hematite. The first set contained the parameters A and ρ of the cobalt-water interaction and the A and ρ of the iron-water interaction. The second set contained the two cobalt parameters and the A and ρ parameters of the $O_{hematite}$-O_{water} interaction. Again, we created a parameter grid of the four parameters in each set by multiplying each parameter A and $1/\rho$ individually with a given factor. For each point on this parameter grid we again calculated the SSD between the DFT energy curve and the energy curve of the grid point, and tried to minimize the value of the SSD.

Figure 13 depicts some of the energy curves with a relatively small SSD, of the order 1.5-2.5 eV^2 for the parameter set that includes the iron-water interaction. Only one of these curves has negative values for the energy, and none of them represent the DFT energy curve. Also, the shape of these curves shows the same behavior we saw with trying fitting the two parameters in Section 4.2. Thus, we again looked at the influence that the two parameters of the iron-water interaction have on the shape of the energy curve. We did this by keeping the cobalt and all the other parameters constant and multiplying only one for the iron-water interaction parameters with a factor between 0.1 and 1.9. Here, we took the rest of the parameters to be the parameters from Table 2. The two comparisons of influence can be found in Figure 14.

Again, the parameters do not seem to have an influence on a shift of the minimum to the left or

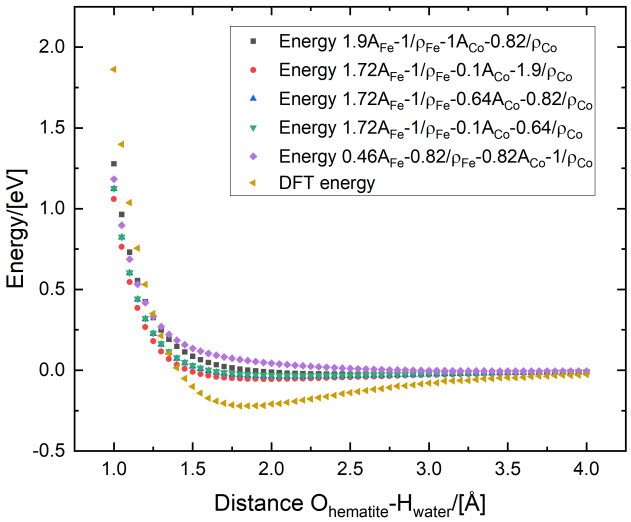

Figure 13: *Some energy curves of minimal SSD values for the cobalt-water and iron-water parameter set. These curves are compared to the DFT energy curve.*

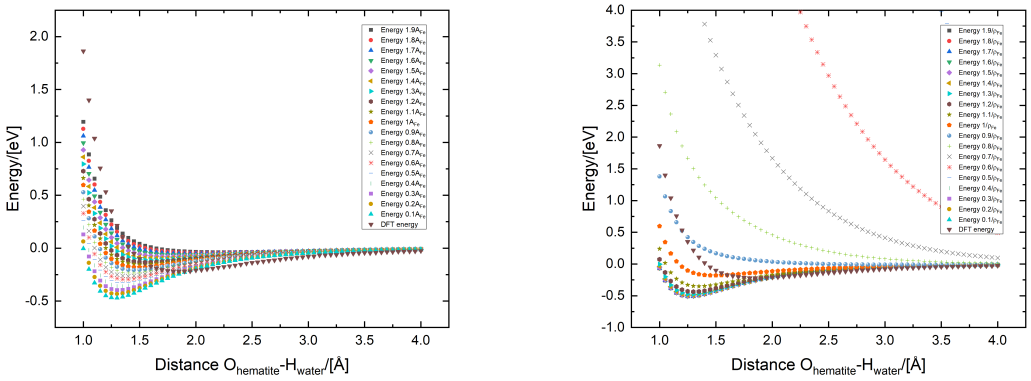

(a) *Comparing A of the iron-water interaction.*

(b) *Comparing ρ of the iron-water interaction.*

Figure 14: *The comparison of the influence of the two different parameters of the iron-water interaction on the energy curves for the cobalt doped hematite.*

right in the plot, but more on the shift up- and downwards. After looking at these influences and trying to fit the parameters, we concluded that this set of parameters can probably not be used to fit the classical energy curve to the DFT energy curve.

Parallel to this fitting, we tried to do the same using the cobalt-water interaction and the interaction between the two oxygens, in the water and in the hematite. For these simulations, we took the parameters of the iron-water interaction to be the ones from the fitted pure hematite. We multiplied the four parameters in the set individually with a factor to create a parameter grid and used the SSD between the resulting energy curve and the DFT energy curve to find the optimal set of parameters. Figure 15 shows the energy curve of the parameters with the minimal SSD on the grid that we considered, with an SSD of the order 0.5 eV^2. This curve does show a minimal, negative value,

although it is not at the same distance between the water and hematite as the DFT curve and it is not as deep.

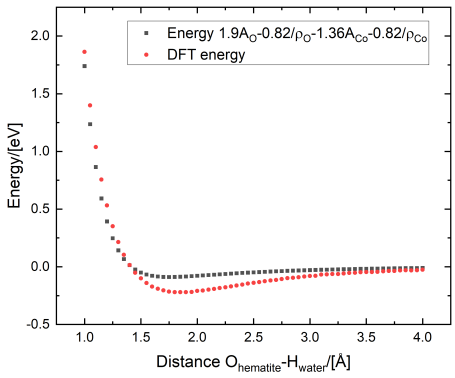

Figure 15: *The energy curve of minimal SSD for the cobalt-water and oxygen-oxygen parameter set. The curve is compared to the DFT energy curve.*

In order to compare this set of parameters to the set that included the iron-water interaction, we also looked at the influence that the two interaction parameters between the oxygen atoms have on the shape of the energy curve. We kept the parameters of the iron and cobalt interaction with the water constant and altered the parameters A and $1/\rho$ of the $O_{hematite}$-O_{water} individually, again by individually multiplying the parameters with a factor between 0.1 and 1.9. This resulted in the energy curves shown in Figure 16.

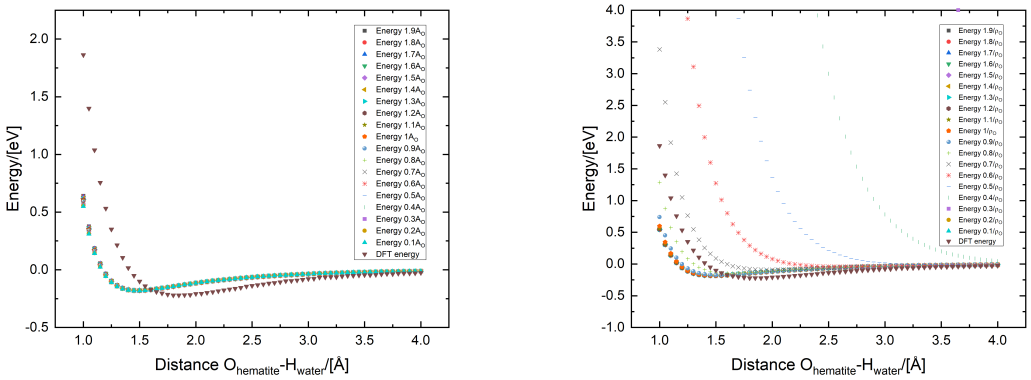

(a) *Comparing A of the oxygen-oxygen interaction.* ***(b)*** *Comparing ρ of the oxygen-oxygen interaction.*

Figure 16: *The comparison of the influence of the two different parameters of the oxygen-oxygen interaction on the energy curves for the cobalt doped hematite.*

The parameters of the oxygen-oxygen interaction again do not show to have much influence on the position of the minimum of the energy curves, but more on the magnitude of the minimum. However, compared to other parameters, the parameter $1/\rho$ of this interaction seems to shift the minimum more to the right in the plot than any of the other parameters that we compared in this way. This indicates that these parameters can still be used to fit the energy curve, but not in combination with only the cobalt-water parameters. Therefore, the next thing we tried is to fit all six parameters, the parameters A and ρ of the three interactions: iron-water, cobalt-water and oxygen-oxygen.

4.4 Fitting six parameters

The last thing we tried for fitting the energy curves, was taking into account six parameters of the force field. These were the parameters A and ρ parameters of the $Fe_{hematite}$-O_{water}, $Co_{hematite}$-O_{water} and $O_{hematite}$-O_{water} interactions. We created a parameter grid by independently multiplying each parameter by a factor. However, since there are six parameters, the computational time can get very big if this grid is too refined. The grid that we used was thus very rough in comparison with previous grids that we used for smaller numbers of parameters, since we could not use a lot of different factors per parameter. Still, some of the energy curves with the minimal SSD from this parameter grid can be found in Figure 17 and they are significantly better than previous energy curves that we tried to fit. These curves have an SSD of the order of magnitude 0.1 eV^2. The minima of both the classical curves and the DFT curve are about 0.1 Å apart, but a more refined grid might fit the classical curves even more accurately to remove this difference. Since some of these curves are practically equal to each other, we took the parameters for the interactions that are closest to the parameters in Table 2. These parameters can be found in Table 3.

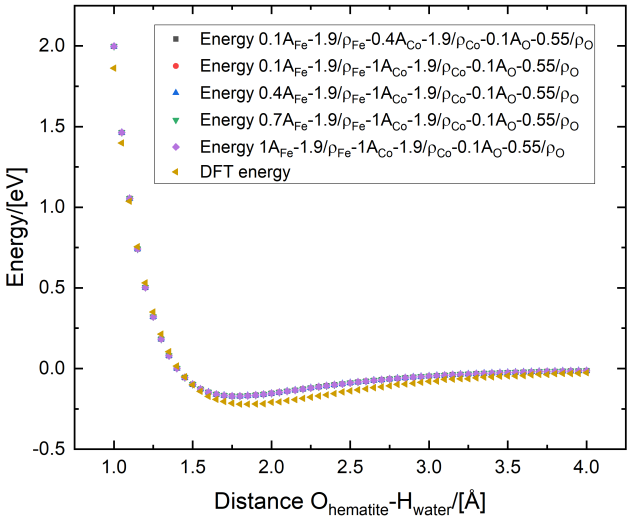

Figure 17: *Some of the energy curve with minimal SSD values for the six parameter set fitting of the cobalt doped hematite. The curves are compared to the DFT energy curve.*

What we concluded from this is that all six parameters are needed to fit the energy curve and a smaller number of parameters is in this case not sufficient. Physically, this shows that the introduction of cobalt into hematite not only introduces an extra interaction of the force field, but also alters the interaction of the other atoms in the hematite with a water molecule.

Table 3: *The fitted parameters of the force field between cobalt doped hematite and a water molecule.*

Interaction	A (eV)	ρ (Å)	C (eV Å^6)
$O_{hematite}$-O_{water}	3414.60	0.270911	28.92
$Fe_{hematite}$-O_{water}	551.25	0.231507	0.0
$O_{hematite}$-H_{water}	495.3375	0.166667	0.0
$Co_{hematite}$-O_{water}	551.25	0.231507	0.0

4.5 Fitting nickel and titanium

With the knowledge that we obtained from trying to fit the parameters for cobalt doped hematite, we set out to do the same for both the nickel and titanium doped hematite. Since the parameters of the iron-water and oxygen-oxygen interaction changed due to the introduction of cobalt, it might indicate that these parameters change because of the introduction of nickel or titanium as well, since these two doped hematites could also not be fitted using just the two interaction parameters between the dopant and the water. Instead of trying to fit the six parameters simultaneously, like we did for the cobalt doped hematite, we first tried to fit the A and ρ parameters for the nickel-water and titanium-water interactions in parallel utilizing the already fitted parameters from the cobalt doped hematite. If this fitting was a success, that would mean that the introduction of a dopant changed the force field of the rest of the hematite, not necessarily which dopant is used. Also, by only trying to fit two parameters we would save time if the fitting was successful.

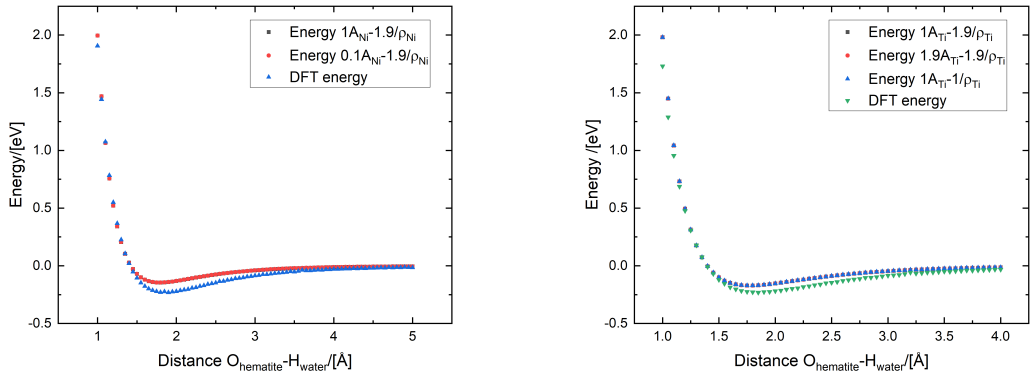

(a) *Nickel* ***(b)*** *Titanium*

Figure 18: *Some of the energy curves with minimal SSD for both nickel and titanium doped hematites compared to their respective DFT curves.*

Figure 18 shows the energy curves where the A and ρ parameters of the dopant-water interaction are fitted, while the other parameters are taken from Table 3. These curves indeed show an agreement with the DFT energy curve, with and SSD for both of the order 0.2 eV^2. This confirms that the introduction of the dopant causes the force field of the rest of the hematite to change, not the type of dopant itself. Again, since the resulting curves of minimal SSD are nearly identical, we chose the parameters of the dopant-water interactions that were closest to the original parameters from Table 2. The new parameters can be found in Table 4.

Table 4: *The interaction parameters of the nickel-water and titanium-water interaction from the two parameter fitting.*

Interaction	A (eV)	ρ (Å)	C (eV Å^6)
$Ni_{hematite}$-O_{water}	551.25	0.231507	0.0
$Ti_{hematite}$-O_{water}	551.25	0.439867	0.0

In order to confirm this and save time on computational time, we tried to fit the six parameters for nickel and titanium in parallel with trying to fit just the two parameters for the dopant-water interactions of nickel and titanium. The curves of the minimal SSD of the grid we chose are depicted in Figure 19, where we compared the resulting curve with the curves that follow from the parameters in Table 4 and the DFT energy curve. Indeed, the resulting curves from fitting six parameters are almost identical to the energy curves from the two parameter fitting, for both the

nickel and titanium. Also the SSDs of the two parameter fitting and six parameter fitting are practically identical.

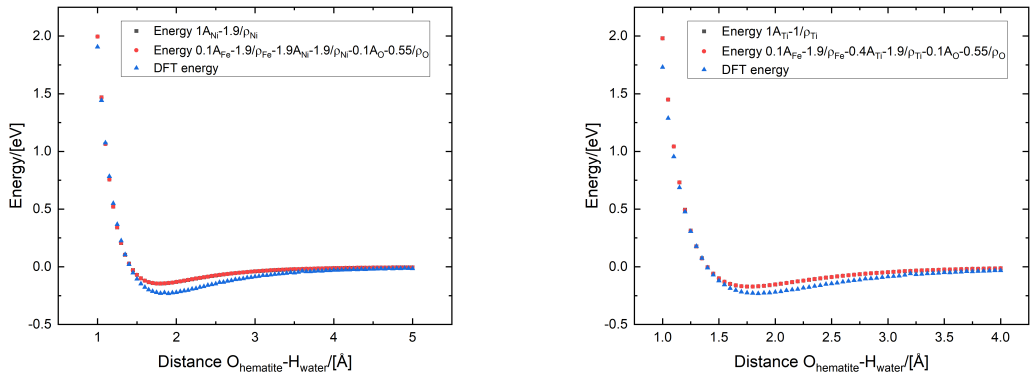

(a) *Nickel* ***(b)*** *Titanium*

Figure 19: *The energy curves of minimal SSD from the six parameter fitting compared to the chosen two parameter fitting curves. Both curves are also compared to the DFT energy curves of both the nickel and titanium doped hematite, respectively.*

We concluded from this that the introduction of the dopant causes a change in the force field of the other atoms in the hematite. In this regard, it does not seem to matter which type of dopant is introduced, since the curves for both the nickel and titanium doped hematite of the two parameters fitting are practically the same as the six parameter fitting curves.

4.6 Molecular diffusion

Once we had the parameters of the force fields for all the different hematites, we could do some molecular dynamics simulations. Unfortunately, due to time restrictions, it was not possible to obtain any results for the different doped hematites. However, with the parameters from Table 3 and Table 4, this could be done. Instead, we focused on the molecular diffusion of water over the surface of pure hematite. We calculated the diffusion coefficient for different numbers of water molecules N distributed over the surface of the pure hematite, in both the x and y direction of the unit cell, i.e. in the parallel plane to the surface. To do this, the mean square displacement (MSD) is calculated as a function of the elapsed time of the simulation. The diffusion coefficients are half of the slopes of the fitted lines through the MSD measurement points that lie in between a value of $(0.5\lambda)^2$ and λ^2. This follows from equation (9). Here, λ is the width of the unit cell in the given direction of the calculation of the diffusion coefficient. We thus got two diffusion coefficients per N, one in the x direction and one in the y direction. One such calculation of the diffusion coefficients for 144 water molecules can be found in Figure 20. The plots of the MSD for the rest of the values for N can be found in Appendix A as log-log plots.

We did this fitting and calculation for different values of N, and we obtained the values for the diffusion coefficients shown in Figure 21.

The errors of the measurement points are partially due to the error obtained from the linear fitting and partly due to the fact that some N had only a few or even less measurement points inside the range of interest. Therefore, we sometimes had to take more points into account than the points that were within the range $(0.5\lambda)^2 - \lambda^2$. We then used the points that visually were on the same line as the points inside the range or interest.

We concluded from this plot that the diffusion of water over the surface of pure hematite decreases as the number of molecules N increases. For larger N the molecules impede each other

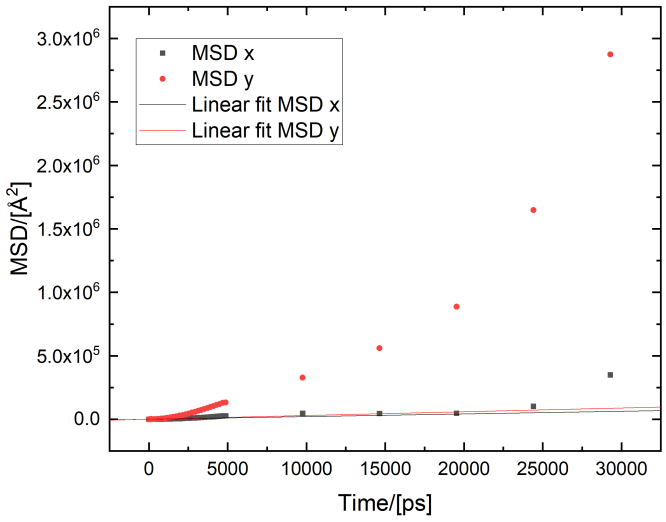

Figure 20: *The fitting of the molecular diffusion coefficients for 144 water molecules.*

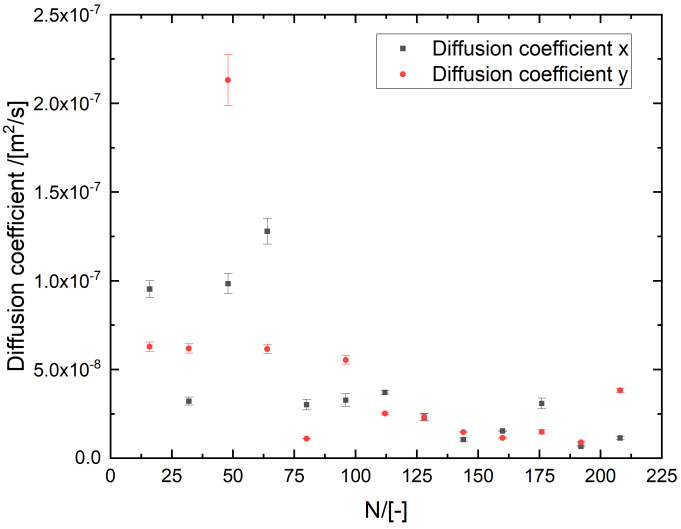

Figure 21: *The diffusion coefficients for both the x and y direction, i.e. the two directions parallel to the surface, as a function of the number of molecules N.*

from diffusing over the surface. For smaller N, around 50 molecules, the water molecules assist each other in diffusing over the surface of the hematite. Also, we see that the trend in the x and y direction are similar, which is what we expected on this geometrically consistent surface.

5 Conclusion

In this report, we sought out to find classical parameters that could replicate the energies calculated using DFT calculations between three different doped hematites and a water molecule. First, we tried to fit the energy curves using only the interaction parameters of the dopant metals with the water molecule. However, these parameters seemed to have no influence on the placement of the energy minimum and could therefore not replicate the DFT energy curves. This means that the introduction of the dopant does not only change the interaction of the atom that it replaced, but also changes some of the other interactions.

In order to find out which interactions are altered as well, we tried to fit the energy curves using two sets of four parameters for only the cobalt doped hematite. Both of these sets contained the interaction parameters of the cobalt with the water and one of the other interactions. The first of these set included the interaction parameters of the iron with the water. This set of parameters could not be used to fit the DFT energy curve. Again, the parameters seem to be not able to shift the minima of the curve further away from the hematite, such that the energy curve was never fitted well. The second set of parameters included the interaction of the oxygen atoms of the hematite with the oxygen atom of water. This set could also not be used to fit the energy curve of the classical force field. However, the parameters in this set shifted the minimum of the energy curve farther away from the hematite, although the effect itself was too small to fit the energy curve.

After this attempt, we tried to fit the energy curve using all six parameters that we used for the two different sets. These parameters could indeed be adjusted so that the subsequent energy curve fitted the DFT energy. Even with the coarse parameter grid that we tried, the best energy curve of this parameter grid had almost the same minimum and magnitude as the DFT energy curve. Also, for every one of the three interactions, at least one of the two parameters had to be adjusted. Thus concluding that the introduction of cobalt into the hematite not only changes the interaction of the replaced atom with the water, but all the interactions of the hematite with the oxygen of the water. The minimum of the classical energy curve with these parameters is still 0.1 Å different from the DFT curve, but this could also be due to the coarse grid that we used for the fitting, and therefore the lack of different values per parameter that we tried. Refining the grid might also fit the curves better.

Lastly, we tried to use our methods from fitting the cobalt doped hematite to the nickel doped hematite and the titanium doped hematite. We tried two different approaches in parallel with each other to find out what the differences between the two are and what the conclusion is that follows from the differences. The first approach was taking the fitted parameters of the cobalt doped hematite and only refitting the parameters of the interaction between the dopant metal and the water. This fitting was visually a good fit, but for comparison we tried to fit these dopant metals also with six parameters. We found that the energy curve of the fitted six parameters was almost equal to the fitting using only the dopant-water interaction. To save time, we could have used only the two parameters, since the two resulting energy curves are near equal. However, now we can conclude that the changing of all interactions is affected by the introduction of a dopant metal, but it does not seem to matter which dopant metal. The parameters of the dopant metal interacting with the water do need to be refitted, but since this involves only two parameters, the fitting is not time consuming compared to fitting six or more parameters.

For the diffusion of water over the surface of pure hematite that the optimal number of molecules is ca. 50 molecules per unit cell. Unfortunately due to time constraints we could not compare this diffusion to the diffusion over the doped hematite surfaces, but this could be a good topic for further research, and we found the parameters that are needed to conduct the needed simulations.

References

[1] P. Liao, M. C. Toroker, and E. A. Carter, "Electron transport in pure and doped hematite," *Nano letters*, vol. 11, no. 4, pp. 1775–1781, 2011.

[2] J. Gutierrez-Sevillano, A. Podsiadły-Paszkowska, B. Szyja, and S. Calero, "On the design of models for an accurate description of the water – hematite interface," *Applied Surface Science*, vol. 560, Sep. 2021.

[3] X.-F. Pang, *Water: molecular structure and properties*. Singapore: World Scientific, 2014.

[4] W. Humphrey, A. Dalke, and K. Schulten, "VMD – Visual Molecular Dynamics," *Journal of Molecular Graphics*, vol. 14, pp. 33–38, 1996.

[5] M. Tarini, P. Cignoni, and C. Montani, "Ambient occlusion and edge cueing for enhancing real time molecular visualization," *IEEE Transactions on Visualization and Computer Graphics*, vol. 12, no. 5, pp. 1237–1244, 2006.

[6] D. Morel, *Hematite : Sources, Properties and Applications.* Nova Science Publishers, Inc, 2013. [Online]. Available: https://search-ebscohost-com.dianus.libr.tue.nl/login.aspx?direct=true&db=nlebk&AN=633009&site=ehost-live

[7] L. E. F. Foa Torres, S. Roche, and J.-C. Charlier, *Electronic Structure Calculations: The Density Functional Theory (DFT)*, 2nd ed. Cambridge University Press, 2020, p. 354–372.

[8] F. Adelchi, F. Stefano, and K. Eckhard, *Introduction To Modern Methods Of Quantum Many-body Theory And Their Applications.*, ser. Series on Advances in Quantum Many-body Theory. World Scientific, 2002, no. v. 7. [Online]. Available: https://search-ebscohost-com.dianus.libr.tue.nl/login.aspx?direct=true&db=nlebk&AN=210693&site=ehost-live

[9] G. Kresse and J. Furthmüller, "Efficient iterative schemes for ab initio total-energy calculations using a plane-wave basis set," Phys. Rev. B, 54 11169-11186, 1996.

[10] G. Kresse and D. Joubert, "From ultrasoft pseudopotentials to the projector augmented-wave method," Phys. Rev. B, 59 1758-1775, 1999.

[11] D. Dubbeldam, "Computer-simulation of adsorption and diffusion of hydrocarbons in zeolites," Ph.D. dissertation, Universiteit van Amsterdam [Host], 2005.

[12] S. Chatterjee, P. G. Debenedetti, F. H. Stillinger, and R. M. Lynden-Bell, "A computational investigation of thermodynamics, structure, dynamics and solvation behavior in modified water models," *The Journal of Chemical Physics*, vol. 128, no. 12, p. 124511, 2008. [Online]. Available: https://doi.org/10.1063/1.2841127

[13] B. M. Szyja and A. Podsiadły-Paszkowska, "Helping thy neighbor: how cobalt doping alters the electrocatalytic properties of hematite," *The journal of physical chemistry letters*, vol. 11, no. 11, pp. 4402–4407, 2020.

[14] F. Cheng and X. Li, "Effects of in situ co or ni doping on the photoelectrochemical performance of hematite nanorod arrays," *Applied Sciences*, vol. 10, no. 10, p. 3567, 2020.

[15] D. Yan, J. Tao, K. Kisslinger, J. Cen, Q. Wu, A. Orlov, and M. Liu, "The role of the domain size and titanium dopant in nanocrystalline hematite thin films for water photolysis," *Nanoscale*, vol. 7, no. 44, pp. 18 515–18 523, 2015.

[16] H. Zakaryan and V. Aroutiounian, "Investigation of cobalt doped tin dioxide structure and defects: Density functional theory and empirical force fields," *Journal of Contemporary Physics (Armenian Academy of Sciences)*, vol. 52, no. 3, pp. 227–233, 2017.

A Diffusion

In this appendix, we show the linear fitting through the log-log plots of the MSD as function of time for all values of N for water over pure hematite surface. We show the log-log plots, while the diffusion coefficients were calculated from the linear-linear plots. The linear fits through the log-log plots indicate the phase of the water, but not the diffusion coefficients. Figure 25 displays the slope for all the linear fitting through the log-log plots. All the values in this figure are near 1 $Å^2/ps$, which means that the behavior of the water is diffusive.

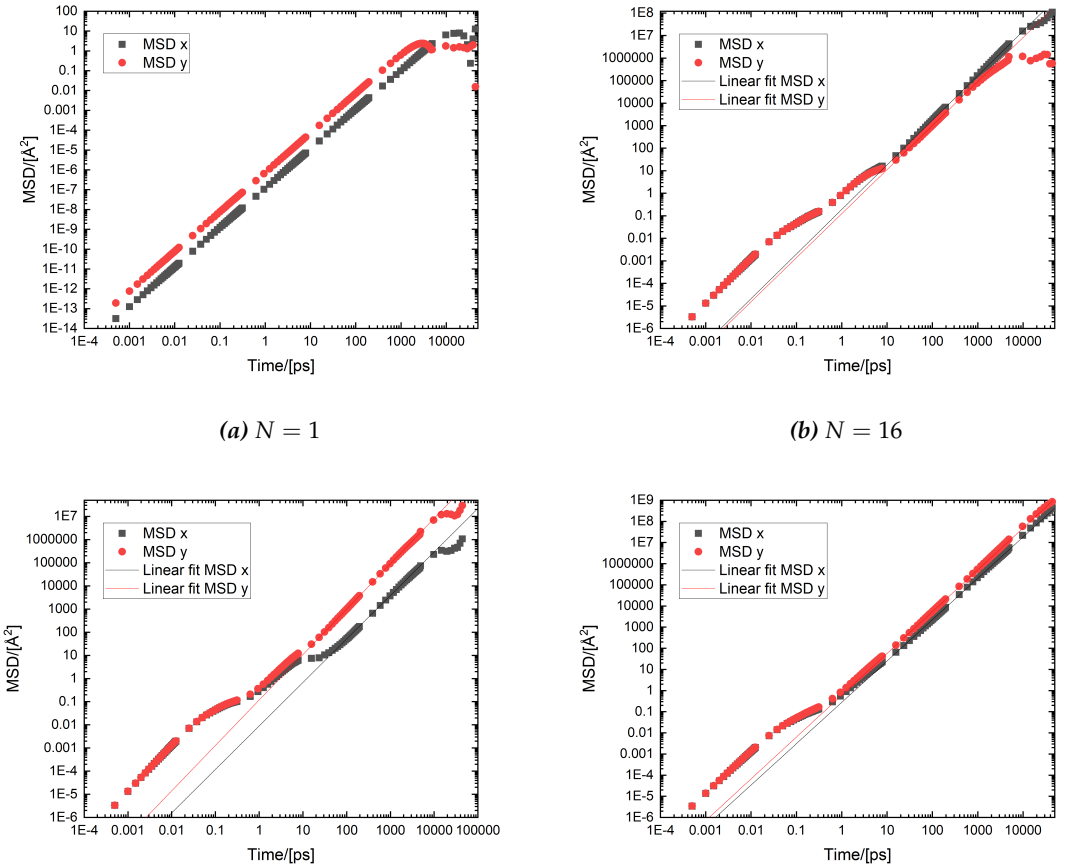

(a) $N = 1$ ***(b)*** $N = 16$

(c) $N = 32$ ***(d)*** $N = 48$

Figure 22: *The log-log plots of the MSD in the x and y direction as function of the time, for some values of N. Also plotted are the linear fits in the $(0.5\lambda)^2 - \lambda^2$ range.*

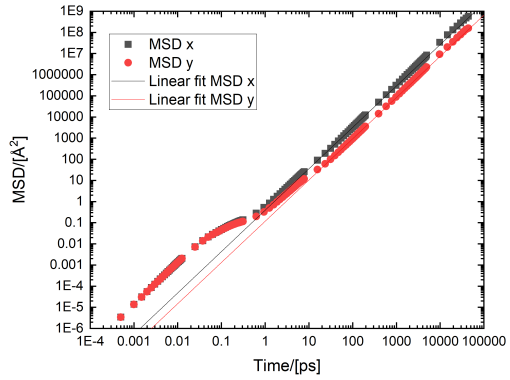

(a) $N = 64$

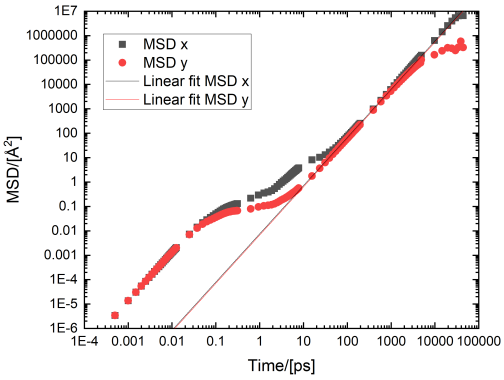

(b) $N = 80$

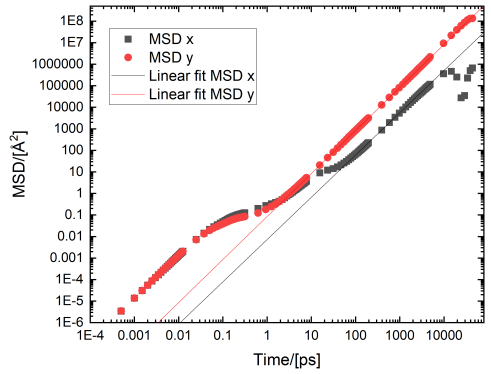

(c) $N = 96$

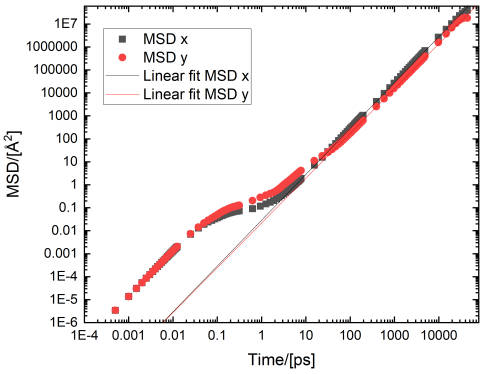

(d) $N = 112$

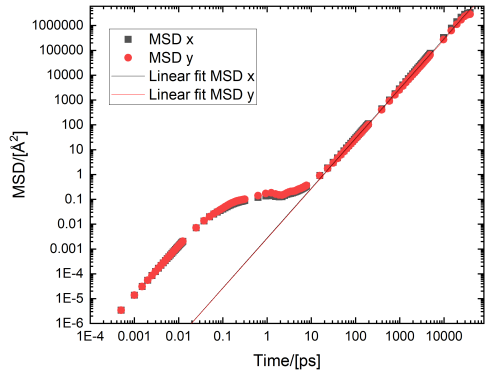

(e) $N = 128$

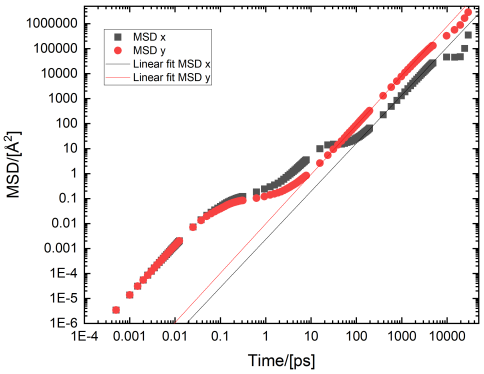

(f) $N = 144$

Figure 23: *The log-log plots of the MSD in the x and y direction as function of the time, for some values of N. Also plotted are the linear fits in the $(0.5\lambda)^2 - \lambda^2$ range.*

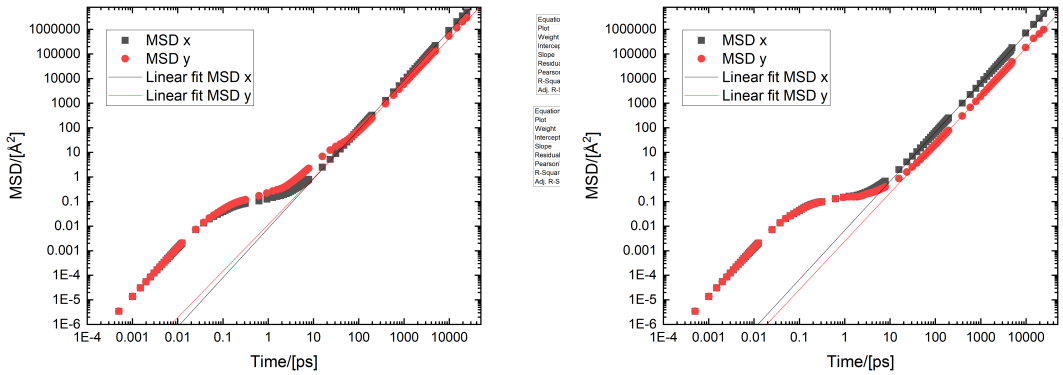

(a) $N = 160$ ***(b)*** $N = 176$

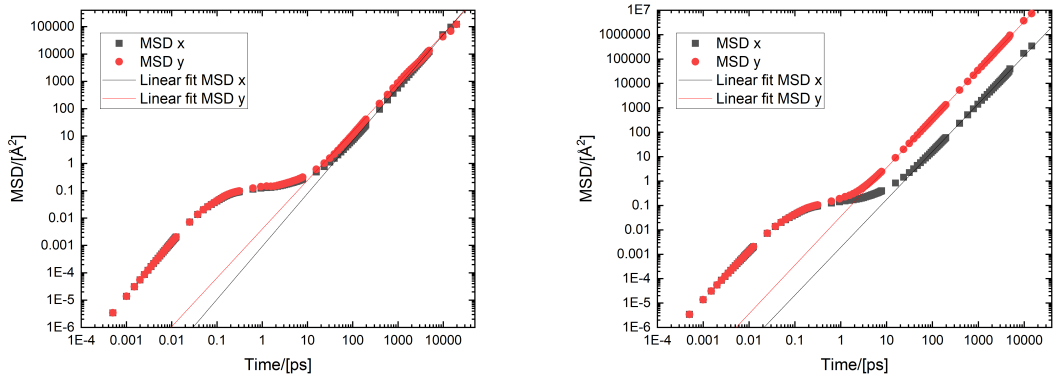

(c) $N = 192$ ***(d)*** $N = 208$

Figure 24: *The log-log plots of the MSD in the x and y direction as function of the time, for some values of N. Also plotted are the linear fits in the* $(0.5\lambda)^2 - \lambda^2$ *range.*

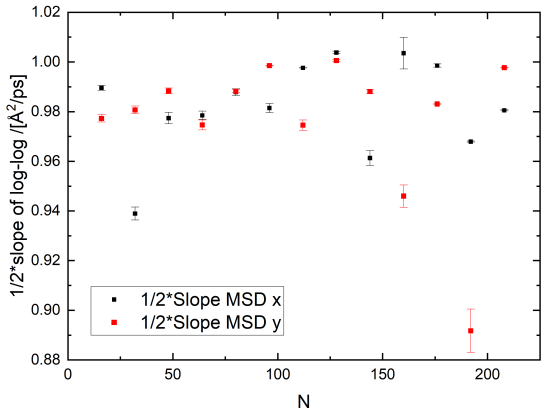

Figure 25: *The values of a half times the slope of the linear fits through the log-log plots for all N.*